Full Length Research Article

# Unveiling the Inhibitory Potential of *Nigella sativa* Phytochemicals Against TG2: Computational and ADMET Approaches for Celiac Disease

https://doi.org/10.62940/als.v13i2.3805

**Issue:** Volume 13, Issue 2 (IN PROGRESS)

**Received:** 09-02-2025

**Revised:** 09-03-2026

**Accepted:** 25-03-2026

**Published online:** 12-06-2026

**Keywords:** Celiac Disease, Molecular Docking, ADME, Molecular Dynamics Simulation, *Nigella sativa*, TG2

**Weam Alyoubi[1], Hani Mohammed Ali[1], Ahmad Firoz[1,*]**

1. Department of Biological Science, Faculty of Science, King Abdul- Aziz University, Jeddah 21589, Saudi Arabia

* aakram@kau.edu.sa

## ABSTRACT

**Background**: Celiac disease (CD) is an autoimmune condition initiated by the ingestion of gluten in individuals with a genetic susceptibility. Transglutaminase 2 (TG2) plays a central role in CD pathogenesis by deamidating gluten peptides, enhancing their immunogenicity. This study explores the inhibitory potential of *Nigella sativa* - derived phytochemicals against TG2.

**Methods**: A library of 132 *Nigella sativa*-derived phytochemicals was screened using molecular docking to identify candidates with high binding affinities for TG2. The top four compounds were further evaluated for pharmacokinetic properties (ADME) and toxicity using SwissADME, admetSAR, pkCSM, and ProTox-II. Molecular dynamics (MD) simulations (100 ns) were conducted to assess the stability of protein- ligand complexes based on RMSD, RMSF, hydrogen bonding, radius of gyration (Rg), and solvent- accessible surface area (SASA).

**Results**: Docking analysis identified four phytochemicals with strong binding affinities to the TG2 active site. ADME and toxicity profiling confirmed favorable drug-like properties and acceptable safety profiles. MD simulations demonstrated stable interactions between TG2 and three of the selected compounds, with consistent binding stability and minimal structural deviations observed throughout the simulations.

**Conclusion** : Three *Nigella sativa* phytochemicals exhibit promising characteristics as potential TG2 inhibitors. These findings provide a computational basis for further experimental validation and development of novel therapies for celiac disease.

# INTRODUCTION

Celiac disease (CD) is a chronic disorder triggered by gluten ingestion in genetically predisposed individuals [1]. CD affects approximately 0.5–1% of the global population, except in regions with low gluten intake and rare predisposing genes [2]. Its development is driven by both genetic and environmental factors, especially gluten exposure [3].

Gluten, a digestion-resistant protein, contains immunogenic peptides that are deamidated by transglutaminase 2 (TG2), enhancing their immunogenicity [4]. In CD, these peptides are presented by antigen-presenting cells via HLA-DQ2/DQ8 molecules, triggering immune responses that can erode the gut lining [5]. Common symptoms include chronic diarrhea, anemia, failure to thrive, malabsorption, weight loss, and abdominal distention [6].

TG2 is a multifunctional protein expressed in various tissues, with calcium-dependent (transamidation, deamidation) and calcium-independent roles. Its dysregulation is implicated in diseases like Huntington's, stroke, Parkinson's, and CD [7]. Three main types of TG2 inhibitors—competitive reversible, non-competitive reversible, and irreversible—have been identified [8,9].

Currently, a strict gluten-free diet (GFD) is the only approved treatment for CD. Nonetheless, alternative therapies are under investigation. Herbal medicine is gaining attention for managing chronic diseases [10,11]. Nigella sativa belongs to the Ranunculaceae family (buttercups) has shown antimicrobial, immunostimulatory, and anti-inflammatory effects. Prior studies suggest its potential in treating gastrointestinal disorders [12], but no comprehensive computational studies have identified TG2 inhibitors from *N. sativa* in CD.

Computational tools are increasingly vital in early drug discovery, enabling virtual screening of compounds [13]. Molecular docking predicts binding affinity and interactions between small molecules and target proteins [14]. However, due to docking's rigidity, combining it with molecular dynamics (MD) simulations offers a better understanding of complex stability under near-physiological conditions [13,15].

# METHODS

### Target Preparation

The 3D crystal structure of transglutaminase 2 (PDB ID: 4PYG) was obtained from the RCSB Protein Data Bank . Non-protein components (ligands, ions, cofactors, and water) were removed using BIOVIA Discovery Studio Visualizer. Missing residues at the N- and C-termini were modeled with MODELLER 10.3. [16]. Hydrogen atoms were added, and Gasteiger charges assigned using AutoDockTools-1.5.7. The prepared structure was saved in .pdbqt format for docking.

### Compound Retrieval and Preparation

*Nigella sativa* was selected for its potential medicinal and biological benefits, as reported in both traditional and modern phytomedicines [17,18]. A total of 132 phytochemicals from *Nigella sativa* were selected based on the availability of structural data (2D/3D formats), relevance to medicinal and pharmacological activity, and uniqueness of chemical scaffolds. These compounds were identified using the LOTUS database, an open-access platform that compiles curated natural product data from multiple ethnobotanical and phytochemical sources [19]. A keyword search using *Nigella sativa* was performed, and compounds with validated natural origin and complete structural information were included (Table S1). The corresponding 3D structures were imported from the PubChem database using SMILES identifiers [20]. Ligands were prepared by assigning AutoDock 4 atom types, setting torsions, identifying aromatic types, and performing energy minimization, hydrogen addition, and charge calculations. All ligands were saved in .pdbqt format. GTP, a known natural inhibitor, was used as a control.

### Identification of Binding Site and Receptor Grid Generation

The active site of an enzyme is the region responsible for substrate binding and catalytic activity [21]. In this study, the GTP binding site of the TG2 enzyme (PDB ID: 4PYG) was targeted, as identified in previous studies [16]. This site is located within a cleft between the first β-barrel and

the catalytic core of the enzyme in its closed conformation [16,22,23]. Based on the identified binding residues, a grid box was defined by setting specific X, Y, and Z dimensions and center coordinates using PyRx with AutoDock Vina for protein–ligand docking [24].

### Docking Analysis

Molecular docking predicts the binding affinity between a target protein and ligands, aiding in drug discovery [25]. Docking was performed using AutoDock Vina via the PyRx platform, which facilitates virtual screening in computer- aided drug design (CADD) [26]. Default parameters were applied. Protein–ligand interactions, including hydrogen bonds and hydrophobic contacts, were visualized and analyzed using PyMOL and BIOVIA Discovery Studio Visualizer.

### PK Properties Prediction

Pharmacokinetic (PK) properties are key factors in assessing a compound's suitability as a drug candidate [27]. These parameters are critical for assessing compound viability during initial drug development stages. In this study, the pharmacokinetic properties of the selected phytochemicals were evaluated using the SwissADME server, an online tool for evaluating pharmacokinetics, drug- likeness, and medicinal chemistry friendliness of small molecules[28,29] .

### Toxicity Prediction

Predicting toxicity is a crucial part of evaluating chemical compounds for safety before clinical trials In this study, the toxicity of the selected compounds was evaluated using the admetSAR, ProTox 3.0, and pkCSM web servers [30]. These tools help estimate various toxicological endpoints, ensuring the safety profile of the compounds. admetSAR provides comprehensive ADMET property predictions based on robust machine learning models [30]. ProTox-II predicts toxicity classes, $LD_{50}$ values, and organ- specific toxicities using chemical similarity and molecular features [31]. pkCSM employs graph- based signatures to predict pharmacokinetic and toxicity properties across a wide range of endpoints [28].

### Molecular Dynamics (MD) Simulations and Trajectory Analysis

MD simulations were conducted using GROMACS with the CHARMM force field to evaluate the stability of protein-ligand complexes [32,33]. Ligand topologies were generated via CGenFF, and each complex was solvated in a dodecahedron box with TIP3P water and neutralized using $Na^+$/$Cl^-$ ions. Energy minimization was performed using the steepest descent algorithm, followed by NVT (100 ps) and NPT (100 ps) equilibration phases. Production simulations were run for 100 ns [34-36] .

Trajectory analyses included RMSD, RMSF, hydrogen bonding, Rg, and SASA providing insight into complex dynamics. All analyses were performed using GROMACS utilities, and results were visualized in Microsoft Excel.

## RESULTS

### Phytochemical Selection and Preparation

A total of 132 Nigella sativa-derived compounds were retrieved from the LOTUS database (Table S1). Their 3D structures were obtained from PubChem in (.sdf) format, then optimized and converted to (.pdbqt) files for docking analysis.

### Binding Site Identification and Grid Box Generation

Based on literature data [16,37], the TG2 inhibitor binding site comprises 13 key amino acid residues . These residues were used to define the grid box in AutoDockTools, with dimensions set to 62 × 50 × 56 and centered at coordinates X = 14.45, Y = −6.98, Z = 2.39 for molecular docking.

### Molecular Docking Analysis

All 132 phytochemicals from *Nigella sativa* were docked against the TG2 protein using AutoDock Vina via the PyRx platform. The docking scores ranged from −8.5 to −4.4 kcal/mol . Based on their superior binding affinities, four top-ranking compounds—CID: 102103091, CID: 136828302, CID: 11402337, and CID: 398941 — were selected for further analysis. These represent approximately the top 3% of the tested compounds. CID: 102103091 exhibited the highest binding score of −8.5 kcal/ mol, surpassing the model ligand GTP (−7.8 kcal/ mol). Detailed docking scores and molecular information of these compounds are presented in Table 1.

### Protein–Ligand Interaction Analysis

Protein– ligand interactions were visualized using BIOVIA Discovery Studio. CID:102103091 formed three hydrogen bonds (ASN586, TYR583, GLU585), one electrostatic interaction (GLU588), and three hydrophobic contacts (ILE591, ARG680, PHE679) (Figure 1 (a) ; Table 2). CID:136828302 formed three hydrogen bonds (TYR583, ASN586, ILE589), two electrostatic interactions (LYS176, GLU588), and one hydrophobic interaction (LYS176) (Figure 1 (b) ; Table 2). CID:11402337 showed two hydrogen bonds (LYS176, ASN177), two electrostatic (LYS176, GLU585), and three hydrophobic contacts (ILE178, LYS176, LYS677) (Figure 1 (c); Table 2). CID:398941 exhibited two hydrogen bonds (LYS176, GLU588) and two hydrophobic interactions (LYS176, PHE679) (Figure 1 (d); Table 2).

### PK Properties

The pharmacokinetic properties of four selected *Nigella sativa* phytochemicals were evaluated using the SwissADME server (Table 3). All compounds had molecular weights (246.26–471.5 g/ mol) and heavy atom counts (18– 34) within acceptable drug-like ranges, indicating moderate complexity. CID:102103091 was the most flexible and exhibited the highest number of hydrogen bond acceptors/ donors and Topological Polar Surface Area (TPSA, 117.42 Å²), suggesting strong protein- binding potential but limited permeability. It also had the highest Molar Refractivity (MR) and lowest lipophilicity (Log P = 0.90), while the other compounds showed moderate lipophilicity (Log P > 2.6), indicating balanced solubility. Water solubility (Log S) ranged from – 2.55 to – 4.32, with CID:11402337 being the most soluble. All compounds demonstrated high gastrointestinal absorption, fulfilled major drug- likeness rules, and had synthetic accessibility scores between 2.51 and 5.28, with CID:102103091 being the most complex. These findings collectively support their favorable pharmacokinetic and Medicinal Chemistry (Medi. Chemistry) profiles.

### Toxicity Prediction

The potential toxicity of the four selected compounds was assessed through in silico analysis using the admetSAR 2.0, pkCSM, and ProTox- II platforms (Table 4). The maximum tolerated dose (MTD) varied, with CID:398941 showing the highest (0.534 log mg/ kg/ day) and CID:136828302 the lowest (−0.425 log mg/kg/ day). Oral rat acute toxicity ($LD_{50}$) values ranged from 1.649 log(mg/kg) (CID:398941) to 2.951 log(mg/kg) (CID:102103091). For chronic toxicity (LOAEL), CID:102103091 had the highest value (3.859 log mg/kg/ day), and CID:136828302 the lowest (1.081 log mg/ kg/ day).All compounds were predicted to be non- carcinogenic, non- mutagenic, non- hepatotoxic, non- cytotoxic, non- AMES toxic, and non- skin sensitizing. In environmental toxicity predictions, CID:102103091 showed the highest toxicity to Tetrahymena pyriformis and fish models. Regarding cardiotoxicity, CID:102103091 and CID:136828302 were predicted to inhibit hERG II channels, while CID:11402337 and CID:398941 showed no hERG I/II inhibition.

### MD Simulations Analysis

### RMSD Analysis

RMSD analysis was conducted to evaluate the equilibration of the protein-ligand complexes over a 100 ns simulation. RMSD values for TG2 alone, TG2-GTP, and TG2 bound to CID: 102103091, 136828302, 11402337, and 398941 were recorded. TG2 alone showed minimal fluctuations between 0.0 and 0.2 nm. TG2- GTP complex initially fluctuated between 0.1 and 0.3 nm, increasing up to 0.4 nm after 50 ns. Among the complexes, TG2– CID: 398941 exhibited RMSD

values between 0.1 and 0.2 nm. CID: 102103091 and 136828302 showed fluctuations up to 0.3 nm. CID: 11402337 remained below 0.3 nm with slight end-point fluctuations (Figure 2 (a)).

Ligand RMSD values were all below 0.3 nm. CID: 136828302, 11402337, and 398941 had more stable ligand RMSD profiles compared to GTP, while CID: 102103091 showed minor changes (Figure 2(b)).

### RMSF Analysis

RMSF values were calculated for TG2 residues across all complexes and unbound TG2. Most residues exhibited low fluctuation. Peaks were noted at residues 1–50, 99–150, 393–442, and 687. RMSF varied from 0.05 to 0.4 nm for most systems, with slight increases at ALA71 for CID: 102103091 and 136828302. The unbound TG2 protein showed lower fluctuations compared to ligand-bound forms ()).

### Hydrogen Bonds (HB)

Hydrogen bond analysis over the 100 ns MD simulation revealed distinct interaction patterns for each complex (Figure 2(d)). CID:102103091 maintained between one and seven hydrogen bonds with slight fluctuations after 40 ns, suggesting stable binding. Similarly, CID: 136828302 formed between one and five hydrogen bonds, exhibiting stable interactions throughout the simulation. The number of hydrogen bonds for CID: 11402337 fluctuates more than other complexes, with values ranging between one and five bonds. CID:398941 formed the fewest hydrogen bonds, reflecting weak interactions. As expected, the control ligand GTP exhibited the highest number of hydrogen bonds, reaching up to twelve, indicating strong binding affinity to TG2.

### Radius of Gyration (Rg)

The Rg values for all protein–ligand complexes remained within 3.00–3.10 nm, showing minor fluctuations throughout the 100 ns simulation, which indicates overall structural stability (Figure 2(e)). The unbound TG2 protein had slightly lower Rg values, ranging from 2.90 to 3.05 nm. The absence of significant spikes in the Rg profiles suggests that ligand binding did not cause major conformational changes, and the overall protein compactness remained stable.

### Solvent Accessible Surface Area (SASA)

SASA values over the simulation (Figure 2(f)) showed that unbound TG2 had the lowest values, fluctuating between 302 and 320 nm². GTP, CID:102103091, and CID:136828302 exhibited higher SASA values, indicating slight expansion and increased solvent exposure upon binding. CID:11402337 and CID:398941 showed intermediate SASA values (310–330 nm²), suggesting moderate surface exposure. The overall stable SASA profiles indicate no significant unfolding or destabilization of TG2 by any ligand.

## Figures

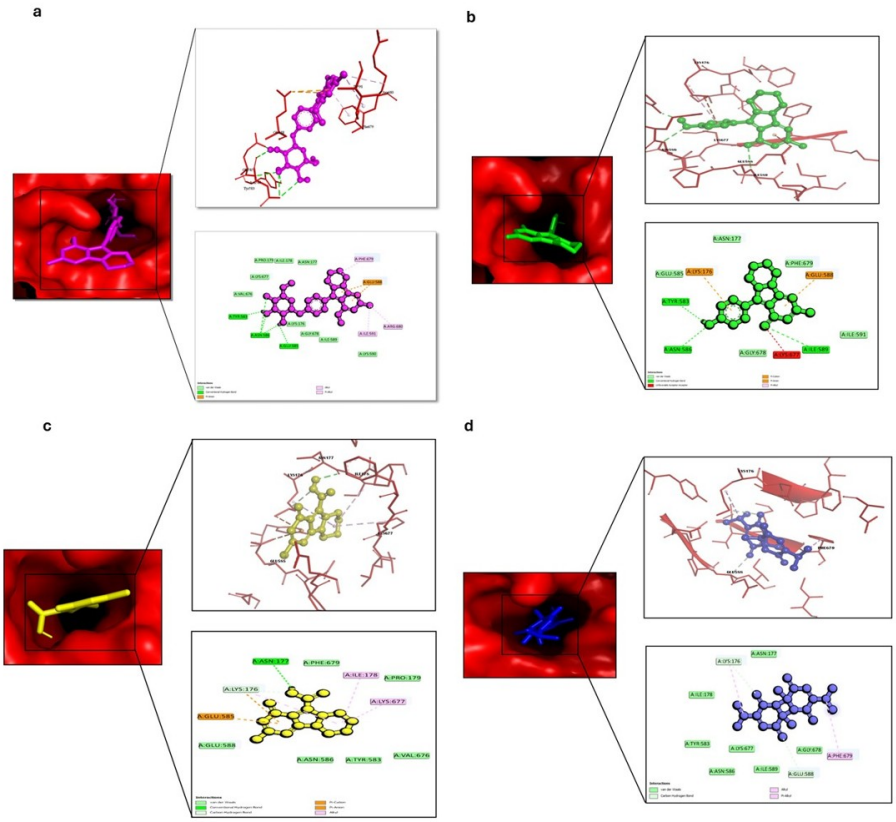


*Figure 1 (a): The interaction between 4PYG and CID:102103091, shown as 3D (top) and 2D (bottom) representations, visualized with BIOVIA Discovery Studio. Figure 1 (b): The interaction between 4PYG and CID:136828302, shown as 3D (top) and 2D (bottom) representations, visualized with BIOVIA Discovery Studio. Figure 1 (c): The interaction between 4PYG and CID:11402337, shown as 3D (top) and 2D (bottom) representations, visualized with BIOVIA Discovery Studio. Figure 1 (d): The interaction between 4PYG and CID:398941, shown as 3D (top) and 2D (bottom) representations, visualized with BIOVIA Discovery Studio.*

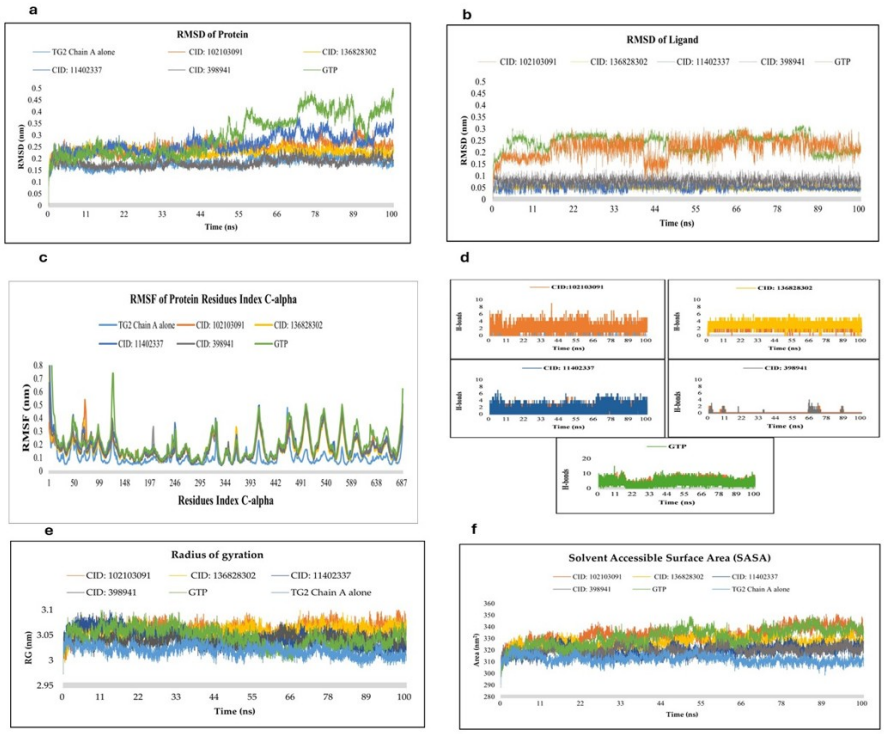


*Figure 2 (a): RMSD of TG2 alone (cyan) and complexes during 100 ns simulation: CID:102103091 (orange), CID:136828302 (yellow), CID:11402337 (blue), CID:398941 (gray), and GTP (green). Figure 2 (b): RMSD of ligands during 100 ns simulation: CID:102103091 (orange), CID:136828302 (yellow), CID:11402337 (blue), CID:398941 (gray), and GTP (green). Figure 2 (c): RMSF of TG2 alone (cyan) and in complexes during 100 ns with CID:102103091 (orange), CID:136828302 (yellow), CID:11402337 (blue), CID:398941 (gray), and GTP (green). Figure 2 (d): H-bond monitoring plot of complexes during 100 ns simulation: CID:102103091 (orange),*

*CID:136828302 (yellow), CID:11402337 (blue), CID:398941 (gray), and GTP (green). Figure 2 (e): The radius of gyration (Rg) of TG2 chain A alone (cyan) and four com-pound complexes during 100 ns simulation with CID:102103091 (orange), CID:136828302 (yellow), CID:11402337 (blue), CID:398941 (gray), and the model lig-and (GTP) (green). Figure 2 (f): Solvent Accessible Surface Area (SASA) of TG2 chain A alone (cyan) and four compound complexes during 100 ns simulation with CID:102103091 (orange), CID:136828302 (yellow), CID:11402337 (blue), CID:398941 (gray), and the model lig-and (GTP) (green).*

## Tables

| PubChem CID | Molecular Formula | 2D Structure | Docking Score (Kcal/mol) |
|---|---|---|---|
| 102103091 | $C_{25}H_{31}N_2O_7^+$ | 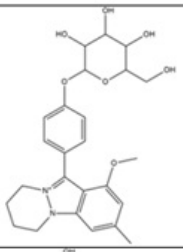 | -8.5 kcal/mol |
| 136828302 | $C_{18}H_{18}N_2O_2$ | 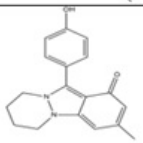 | -7.7 kcal/mol |
| 11402337 | $C_{13}H_{14}N_2O_3$ | 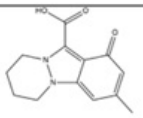 | -7.1 kcal/mol |
| 398941 | $C_{20}H_{24}O_4$ | 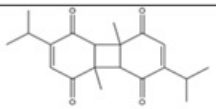 | -6.9 kcal/mol |
| Model ligand (GTP) 135398633 | $C_{10}H_{16}N_5O_{14}P_3$ | 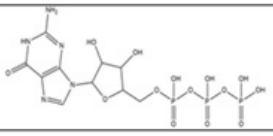 | -7.8 kcal/mol |

*Table 1: PubChem CID, Molecular Formula, 2D Structure, and Docking Scores of the Top Four Natural Compounds from Nigella sativa and the Control Ligand (GTP).*

| Compound | Category | Residues | Bond distance (Å) |
|---|---|---|---|
| CID:102103091 | Hydrogen Bonds | ASN586 | 2.957 |
| | | TYR583 | 2.189 |
| | | GLU585 | 2.239 |
| | Electrostatic | GLU588 | 4.409 |
| | Hydrophobic Interactions | ILE591 | 4.148 |
| | | ARG680 | 4.355 |
| | | PHE679 | 4.941 |
| CID: 136828302 | Hydrogen Bond | TYR583 | 2.094 |
| | | ASN586 | 3.108 |
| | | ILE589 | 3.125 |
| | Electrostatic | LYS176 | 4.540 |
| | | GLU588 | 4.188 |
| | Hydrophobic | LYS176 | 5.425 |
| CID: 11402337 | Hydrogen Bond | ASN177 | 2.424 |
| | | LYS176 | 3.463 |
| | Electrostatic | LYS176 | 4.225 |
| | | GLU585 | 4.086 |
| | Hydrophobic | ILE178 | 5.318 |
| | | LYS176 | 5.071 |
| | | LYS677 | 4.811 |
| CID: 398941 | Hydrogen Bonds | LYS176 | 3.432 |
| | | GLU588 | 3.250 |
| | Hydrophobic Interactions | LYS176 | 4.469 |
| | | PHE679 | 4.666 |

*Table 2: Protein-Ligand Interactions from Docking Analysis.*

| Properties | | CID: 102103091 | CID: 136828302 | CID: 11402337 | CID: 398941 |
|---|---|---|---|---|---|
| Physicochemical | MW (g/mol) | 471.5 | 294.35 | 246.26 | 328.4 |
| | Heavy atoms | 34 | 22 | 18 | 24 |
| | Arom. heavy atoms | 15 | 15 | 9 | 0 |
| | Rotatable bonds | 5 | 1 | 1 | 2 |
| | H-bond acceptors | 7 | 2 | 3 | 4 |
| | H-bond donors | 4 | 1 | 1 | 0 |
| | TPSA | 117.42Å² | 47.16 Å² | 64.23 Å² | 68.28 Å² |
| | MR | 125.65 | 88.65 | 68.15 | 91.24 |
| Lipophilicity | Log Po/w | 0.90 | 2.82 | 2.82 | 2.62 |
| Water Solubility | Log S (ESOL) | -4.32 | -3.95 | -2.55 | -3.05 |
| Pharmacokinetics | GI absorption | High | High | High | High |
| Drug-likeness | Lipinski | Yes | Yes | Yes | Yes |
| | Ghose | Yes | Yes | Yes | Yes |
| | Veber | Yes | Yes | Yes | Yes |
| | Egan | Yes | Yes | Yes | Yes |
| | Muegge | Yes | Yes | Yes | Yes |
| Medi. Chemistry | Synthetic accessibility | 5.28 | 2.86 | 2.51 | 4.65 |

*Table 3: PK Properties of the Top Four Nigella sativa Compounds.*

| Parameters | CID:102103091 | CID: 136828302 | CID: 11402337 | CID: 398941 |
|---|---|---|---|---|
| Max. tolerated dose (Human) (log mg/kg/day) | 0.276 | -0.425 | 0.283 | 0.534 |
| Oral rat acute toxicity LD50 (log mg/kg) | 2.951 | 2.423 | 2.265 | 1.649 |
| Oral Rat Chronic Toxicity (LOAEL) (log mg/kg/day) | 3.859 | 1.081 | 1.17 | 1.53 |
| Hepatotoxicity | In | In | In | In |
| Carcinogenicity | In | In | In | In |
| Mutagenicity | In | In | In | In |
| Cytotoxicity | In | In | In | In |
| AMES toxicity | In | In | In | In |
| Skin sensitization | No | No | No | No |
| T. pyriformis toxicity (log mmol/L) | 0.285 | 1.437 | 0.237 | 0.445 |
| Minnow toxicity (log mmol/L) | 2.528 | 1.17 | 1.776 | 1.323 |
| hERG I inhibition | No | No | No | No |
| hERG II inhibition | Yes | Yes | No | No |

*Table 4: Overview of Toxicity Parameters for the Four Selected Compounds. "In." stands for inactive, and "Ac." represents active.*

## DISCUSSION

Celiac disease (CD) is an autoimmune disorder triggered by gluten in genetically predisposed individuals, where transglutaminase 2 (TG2) plays a key role by deamidating gluten peptides [38]. Although a gluten-free diet is the only current therapy, it is difficult to maintain and does not prevent all complications [38,39]. Thus, TG2 inhibition offers a promising therapeutic strategy. In this study, it was utilized to assess the binding potential of 132 phytochemicals from *Nigella sativa* against TG2.

Molecular docking is a widely adopted computational technique used to predict the interaction between target proteins and small molecules [40]. CID:102103091 emerged as the top candidate, forming strong hydrogen bonds and hydrophobic contacts, notably with GLU585 and TYR583, indicating strong affinity and specificity. CID:136828302 and CID:11402337 also showed favorable interactions, while CID:398941 exhibited weaker but stable binding, suggesting it may serve as a secondary inhibitor. Similar high-affinity interactions with TG2 have been reported in previous in silico studies, particularly with residues such as GLU585 and TYR583, supporting the potential of small-molecule inhibitors from natural sources [41].

Pharmacokinetic (PK) analysis further supported the drug- likeness of these compounds. CID:102103091, although potent, showed high TPSA and synthetic complexity, which may affect permeability and development. In contrast, CID:11402337 had balanced solubility and lipophilicity, making it a promising oral drug candidate. All four compounds passed major drug-likeness filters, indicating their potential for further optimization. These pharmacokinetic properties are consistent with earlier findings, where *Nigella sativa*- derived phytochemicals

demonstrated acceptable drug-likeness, permeability, and oral bioavailability, indicating their therapeutic viability [42].

Toxicity predictions revealed CID:398941 had the highest MTD, suggesting good tolerance, while CID:136828302 showed the lowest MTD and LOAEL, requiring careful dosing. CID:102103091 had the highest LD50, indicating low acute toxicity, but showed potential environmental risks. Notably, CID:102103091 and CID:136828302 were predicted to inhibit hERG II, suggesting a possible cardiotoxicity risk and warranting further preclinical safety assessment. The predicted low toxicity of the selected compounds aligns with previous computational studies supporting the safety of *Nigella sativa* derivatives [43].

Molecular dynamics (MD) simulations over 100 ns confirmed the complexes' stability. RMSD values remained low, reflecting minimal structural deviation. CID:398941 showed RMSD patterns similar to unbound TG2, suggesting minimal conformational changes. RMSF analysis showed typical flexibility, with minor fluctuations in CID:102103091 and CID:136828302 complexes that did not affect structural integrity.

Hydrogen bonding analysis supported the docking results, with CID:102103091 forming the most consistent bonds. CID:398941 showed fewer hydrogen bonds, aligning with its weaker binding. Rg values remained stable across all complexes, and SASA results indicated minor increases in solvent exposure without compromising protein compactness. Overall, CID:102103091 demonstrated the strongest and most stable interaction profile, suggesting its potential as a TG2 inhibitor for further development.

However, while these phytochemicals show promise, long-term use may impact nutrient absorption or interact with existing celiac disease treatments. Their effects alongside a gluten-free diet remain unclear and warrant further clinical investigation.

This study highlights the potential of *Nigella sativa*-derived phytochemicals as TG2 Inhibitors. Through molecular docking and ADMET analysis, four compounds — CID: 102103091, CID: 136828302, CID: 11402337, and CID: 398941 — were identified with promising binding affinities and favorable pharmacokinetic profiles. Molecular dynamics simulations over 100 ns confirmed the stability of the protein-ligand complexes, especially for CID: 102103091, CID: 136828302, and CID: 11402337.

These findings suggest that *Nigella sativa* phytochemicals could serve as potential TG2 inhibitors and may offer a novel therapeutic avenue for celiac disease. Nonetheless, additional in vitro and in vivo investigations are necessary to evaluate their metabolism, bioavailability, and safety after oral administration.

## FUNDING STATEMENT

No external funding was received for this research.

## CONFLICT OF INTEREST

The authors confirm that they have no conflicts of interest to disclose.

## AUTHOR CONTRIBUTIONS

Weam Alyoubi performed literature review, methodology, data analysis, interpretation of results, and manuscript writing; Hani Mohammed Ali contributed to supervision, methodological guidance, and manuscript review; Ahmad Firoz designed the project, contributed to supervision, interpretation of results, result validation, manuscript writing, and final approval of the submitted version.

### Supplementary data

The following supplementary materials provided are accessible on request.

List of 132 compounds from *Nigella sativa* generated during the virtual screening process, along with their binding affinities (kcal/mol).

## REFERENCES

1. Leonard MM, Sapone A, Catassi C, Fasano A. Celiac disease and nonceliac gluten sensitivity: a review. JAMA, (2017); 318(7): 647-656.
2. Caio G, Volta U, Sapone A, Leffler DA, De Giorgio R, et al. Celiac disease: a comprehensive current review. BMC medicine, (2019); 17(1): 142.
3. Serena G, Lima R, Fasano A. Genetic and environmental contributors for celiac disease. Current Allergy and Asthma Reports, (2019); 191-10.
4. McAllister BP, Williams E, Clarke K. A comprehensive review of celiac disease/gluten-sensitive enteropathies. Clinical reviews in allergy & immunology, (2019); 57: 226-243.
5. Yu XB, Uhde M, Green PH, Alaedini A. Autoantibodies in the extraintestinal manifestations of celiac disease. Nutrients, (2018); 10(8): 1123.
6. Green PHR, Paski S, Ko CW, Rubio-Tapia A. AGA Clinical Practice Update on Management of Refractory Celiac Disease: Expert Review. Gastroenterology, (2022);163(5):1461-1469.
7. Rauhavirta T, Hietikko M, Salmi T, Lindfors K. Transglutaminase 2 and transglutaminase 2 autoantibodies in celiac disease: a review. Clinical reviews in allergy & immunology, (2019); 57(1): 23-38.
8. Jasim MH, Rathbone DL. Reaction profiling of a set of acrylamide-based human tissue transglutaminase inhibitors. Journal of molecular graphics & modelling
9. Yakubov B, Chen L, Belkin AM, Zhang S, Chelladurai B, Zhang Z-Y, et al. Small Molecule Inhibitors Target the Tissue Transglutaminase and Fibronectin Interaction. PLoS ONE (2014); 9(2): e89285.
10. Kumar A, P N, Kumar M, Jose A, Tomer V, et al. Major phytochemicals: recent advances in health benefits and extraction method. Molecules, (2023); 28(2): 887.
11. Nortjie E, Basitere M, Moyo D, Nyamukamba P. Extraction methods, quantitative and qualitative phytochemical screening of medicinal plants for antimicrobial textiles: a review. Plants, (2022); 11(15): 2011.
12. Zakir F, Mishra H, Azharuddin M, Mirza MA, Aggarwal G, et al. Gastrointestinal abnormalities and Nigella sativa: A narrative review of preclinical and clinical studies. Black Seeds (Nigella Sativa), (2022); 355-386.
13. Santos LH, Ferreira RS, Caffarena ER. Integrating molecular docking and molecular dynamics simulations. Docking screens for drug discovery, (2019); 13-34.
14. Shaker B, Ahmad S, Lee J, Jung C, Na D. In silico methods and tools for drug discovery. Computers in biology and medicine, (2021); 137104851.
15. Vidal-Limon A, Aguilar-Toalá JE, Liceaga AM. Integration of molecular docking analysis and molecular dynamics simulations for studying food proteins and bioactive peptides. Journal of agricultural and food chemistry, (2022); 70(4): 934-943.
16. Jang T-H, Lee D-S, Choi K, Jeong EM, Kim I-G, et al. Crystal structure of transglutaminase 2 with GTP complex and amino acid sequence evidence of evolution of GTP binding site. PloS one, (2014); 9(9): e107005.
17. Osman M & Kutty M. Immunotherapeutic Application of Nigella sativa Oil in Management of Dermatitis Herpetiformis Associated with Refractory Coeliac Disease. Research Journal of Pharmaceutical, Biological and Chemical Sciences, (2013); 4: 1181-1186.
18. Osman MT, Al-Duboni G, Taha BI, Muhamed LA. Refractory coeliac disease; role of Nigella sativa as immunomodulator. British Journal of Medicine and Medical Research, (2012); 2(4): 527.
19. Rutz A, Sorokina M, Galgonek J, Mietchen D, Willighagen E, et al. The LOTUS initiative for open knowledge management in natural products research. elife, (2022); 11e70780.
20. Weininger D. SMILES, a chemical language and information system. 1. Introduction to methodology and encoding rules. Journal of chemical information and computer sciences, (1988); 28(1): 31-36.
21. Zhang Z, Li Y, Lin B, Schroeder M, Huang B. Identification of cavities on protein surface using multiple computational approaches for drug binding site prediction. Bioinformatics, (2011); 27(15): 2083-2088.
22. Pinkas DM, Strop P, Brunger AT, Khosla C. Transglutaminase 2 undergoes a large conformational change upon activation. PLoS biology, (2007); 5(12): e327.
23. Lee CS, Park HH. Structural aspects of transglutaminase 2: functional, structural, and regulatory diversity. Apoptosis, (2017); 221057-1068.
24. Dallakyan S, Olson AJ. Small-molecule library screening by docking with PyRx. Chemical biology: methods and protocols, (2015); 243-250.
25. Ghahremanian S, Rashidi MM, Raeisi K, Toghraie D. Molecular dynamics simulation approach for discovering potential inhibitors against SARS-CoV-2: A structural review. Journal of Molecular Liquids, (2022); 118901.
26. Mohammad T, Mathur Y, Hassan MI. InstaDock: A single-click graphical user interface for molecular docking-based virtual high-throughput screening. Briefings in Bioinformatics, (2021); 22(4): bbaa279.
27. Umar AB, Uzairu A, Shallangwa GA, Uba S. Design of potential anti-melanoma agents against SK-MEL-5 cell line using QSAR modeling and molecular docking methods. SN Applied Sciences, (2020); 2(5): 815.
28. Azzam KA. SwissADME and pkCSM webservers predictors: An integrated online platform for accurate and comprehensive predictions for in silico ADME/T properties of artemisinin and its derivatives. Kompleksnoe Ispolzovanie Mineralnogo Syra= Complex use of mineral resources, (2023); 325(2): 14-21.
29. Daina A, Michielin O, Zoete V. SwissADME: a free web tool to evaluate pharmacokinetics, drug-likeness and medicinal chemistry friendliness of small molecules. Scientific reports, (2017); 7(1): 42717.
30. Cheng F, Li W, Zhou Y, Shen J, Wu Z, et al. (2012) admetSAR: a comprehensive source and free tool for assessment of chemical ADMET properties. ACS Publications.
31. Banerjee P, Kemmler E, Dunkel M, Preissner R. ProTox 3.0: a webserver for the prediction of toxicity of chemicals. Nucleic Acids Research, (2024); 52(W1): W513-W520.

32. Filipe HA, Loura LM. Molecular dynamics simulations: advances and applications. Molecules, (2022); 27(7): 2105.
33. Yekeen AA, Durojaye OA, Idris MO, Muritala HF, Arise RO. CHAPERONg: A tool for automated GROMACS-based molecular dynamics simulations and trajectory analyses. Biorxiv, (2023); 2023.2007. 2001.546945.
34. Godwin RC, Melvin R, Salsbury FR. Molecular dynamics simulations and computer-aided drug discovery. Computer-aided drug discovery, (2016); 1-30.
35. Shukla R, Tripathi T. Molecular dynamics simulation of protein and protein–ligand complexes. Computer-aided drug design, (2020); 133-161.
36. Yu H, Dalby PA (2020) A beginner's guide to molecular dynamics simulations and the identification of cross-correlation networks for enzyme engineering. Methods in enzymology: Elsevier. pp. 15-49.
37. Parvatikar PP, Madagi SB. Molecular docking analysis: interaction studies of natural compounds with human TG2 protein; 2020. Springer. pp. 101-111.
38. Caio G, Volta U, Sapone A, Leffler DA, De Giorgio R, et al. Celiac disease: a comprehensive current review. BMC medicine, (2019); 171-20.
39. Yoosuf S, Makharia GK. Evolving therapy for celiac disease. Frontiers in pediatrics, (2019); 7193.
40. Morris CJ, Corte DD. Using molecular docking and molecular dynamics to investigate protein-ligand interactions. Modern Physics Letters B, (2021); 35(08): 2130002.
41. Ahmad S, Abbasi HW, Shahid S, Gul S, Abbasi SW. Molecular docking, simulation and MM-PBSA studies of nigella sativa compounds: a computational quest to identify potential natural antiviral for COVID-19 treatment. Journal of Biomolecular Structure and Dynamics, (2021); 39(12): 4225-4233.
42. Nurhan AD, Gani MA, Budiatin AS, Siswodihardjo S, Khotib J. Molecular docking studies of Nigella sativa L and Curcuma xanthorrhiza Roxb secondary metabolites against histamine N-methyltransferase with their ADMET prediction. Journal of Basic and Clinical Physiology and Pharmacology, (2021); 32(4): 795-802.
43. Dalli M, Bekkouch O, Azizi S-e, Azghar A, Gseyra N, et al. Nigella sativa L. phytochemistry and pharmacological activities: A review (2019–2021). Biomolecules, (2021); 12(1): 20.